

Ridge waveguide lasers in Nd:GGG crystals produced by swift carbon ion irradiation and femtosecond laser ablation

Yuechen Jia,¹ Ningning Dong,¹ Feng Chen,^{1,*} Javier R. Vázquez de Aldana,² Sh. Akhmadaliev,³ and Shengqiang Zhou³

¹*School of Physics, Key Laboratory of Particle Physics and Particle Irradiation (MOE) and State Key Laboratory of Crystal Materials, Shandong University, Jinan 250100, China*

²*Laser Microprocessing Group, Universidad de Salamanca, Salamanca 37008, Spain*

³*Institute of Ion Beam and Materials Research, Helmholtz-Zentrum Dresden-Rossendorf, Dresden D-01314, Germany*

*drfchen@sdu.edu.cn

Abstract: We report on the fabrication of ridge waveguide in Nd:GGG crystal by using swift C⁵⁺ ion irradiation and femtosecond laser ablation. At room temperature continuous wave laser oscillation at wavelength of ~1063 nm has been realized through the optical pump at 808 nm with a slope efficiency of 41.8% and the pump threshold is 71.6 mW.

©2012 Optical Society of America

OCIS codes: (230.7370) Waveguides; (140.3390) Laser materials processing; (130.3120) Integrated optics devices.

References and links

1. N. V. Baburin, B. I. Galagan, Y. K. Danileiko, N. N. Il'ichev, A. V. Masalov, V. Y. Molchanov, and V. A. Chikov, "Two-frequency mode-locked lasing in a monoblock diode-pumped Nd³⁺:GGG laser," *IEEE Quantum Electron.* **31**(4), 303–304 (2001).
2. L. J. Qin, D. Y. Tang, G. Q. Xie, C. M. Dong, Z. T. Jia, and X. T. Tao, "High-power continuous wave and passively Q-switched laser operations of a Nd:GGG crystal," *Laser Phys. Lett.* **5**(2), 100–103 (2008).
3. E. J. Murphy, *Integrated optical circuits and components: Design and applications* (Marcel Dekker, New York, 1999).
4. C. Grivas, "Optically pumped planar waveguide lasers, Part I: Fundamentals and fabrication techniques," *Prog. Quantum Electron.* **35**(6), 159–239 (2011).
5. J. I. Mackenzie, "Dielectric solid-state planar waveguide lasers: A review," *IEEE J. Sel. Top. Quantum Electron.* **13**(3), 626–637 (2007).
6. M. Pollnau, C. Grivas, L. Laversenne, J. S. Wilkinson, R. W. Eason, and D. P. Shepherd, "Ti:Sapphire waveguide lasers," *Laser Phys. Lett.* **4**(8), 560–571 (2007).
7. F. Chen, "Construction of two-dimensional waveguides in insulating optical materials by means of ion beam implantation for photonic applications: Fabrication methods and research progress," *Crit. Rev. Solid State Mater. Sci.* **33**(3-4), 165–182 (2008).
8. F. Chen, X. L. Wang, and K. M. Wang, "Development of ion-implanted optical waveguides in optical materials: A review," *Opt. Mater.* **29**(11), 1523–1542 (2007).
9. F. Chen, "Micro- and submicrometric waveguiding structures in optical crystals produced by ion beams for photonic applications," *Laser Photon. Rev.* DOI 10.1002/lpor.201100037.
10. S. J. Field, D. C. Hanna, A. C. Large, D. P. Shepherd, A. C. Tropper, P. J. Chandler, P. D. Townsend, and L. Zhang, "Ion-implanted Nd:GGG channel waveguide laser," *Opt. Lett.* **17**(1), 52–54 (1992).
11. Y. Y. Ren, N. N. Dong, Y. Tan, J. Guan, F. Chen, and Q. M. Lu, "Continuous wave laser generation in proton implanted Nd:GGG planar waveguides," *J. Lightwave Technol.* **28**, 3578–3581 (2010).
12. C. Zhang, N. N. Dong, J. Yang, F. Chen, J. R. Vázquez de Aldana, and Q. M. Lu, "Channel waveguide lasers in Nd:GGG crystals fabricated by femtosecond laser inscription," *Opt. Express* **19**(13), 12503–12508 (2011).
13. Y. C. Yao, N. N. Dong, F. Chen, S. K. Vanga, and A. A. Bettiol, "Proton beam writing of Nd:GGG crystals as new waveguide laser sources," *Opt. Lett.* **36**(21), 4173–4175 (2011).
14. J. Manzano, J. Olivares, F. Agulló-López, M. L. Crespillo, A. Morono, and E. Hodgson, "Optical waveguides obtained by swift-ion irradiation on silica (a-SiO₂)," *Nucl. Instrum. Methods Phys. Res. B* **268**(19), 3147–3150 (2010).
15. J. Olivares, A. García-Navarro, G. García, A. Méndez, F. Agulló-López, A. García-Cabañes, M. Carrascosa, and O. Caballero, "Nonlinear optical waveguides generated in lithium niobate by swift-ion irradiation at ultralow fluences," *Opt. Lett.* **32**(17), 2587–2589 (2007).
16. P. Kumar, S. M. Babu, S. Ganesamoorthy, A. K. Karnal, and D. Kanjilal, "Influence of swift ions and proton implantation on the formation of optical waveguides in lithium niobate," *J. Appl. Phys.* **102**(8), 084905 (2007).

17. Y. Y. Ren, N. N. Dong, Y. C. Jia, L. L. Pang, Z. G. Wang, Q. M. Lu, and F. Chen, "Efficient laser emissions at 1.06 μm of swift heavy ion irradiated Nd:YCOB waveguides," *Opt. Lett.* **36**(23), 4521–4523 (2011).
18. Y. Y. Ren, N. N. Dong, F. Chen, A. Benayas, D. Jaque, F. Qiu, and T. Narusawa, "Swift heavy-ion irradiated active waveguides in Nd:YAG crystals: fabrication and laser generation," *Opt. Lett.* **35**(19), 3276–3278 (2010).
19. A. García-Navarro, J. Olivares, G. García, F. Agulló-López, S. García-Blanco, C. Merchant, and J. S. Aitchison, "Fabrication of optical waveguides in KGW by swift heavy ion beam irradiation," *Nucl. Instrum. Meth. B.* **249**(1-2), 177–180 (2006).
20. F. Qiu and T. Narusawa, "Application of swift and heavy ion implantation to the formation of chalcogenide glass optical waveguides," *Opt. Mater.* **33**(3), 527–530 (2011).
21. F. Chen, "Photonic guiding structures in lithium niobate crystals produced by energetic ion beams," *J. Appl. Phys.* **106**(8), 081101 (2009).
22. P. D. Townsend, P. J. Chandler, and L. Zhang, *Optical Effects of Ion Implantation* (Cambridge Univ. Press, Cambridge, UK 1994).
23. S. Juodkazis, V. Mizeikis, and H. Misawa, "Three-dimensional microfabrication of materials by femtosecond lasers for photonics applications," *J. Appl. Phys.* **106**(5), 051101 (2009).
24. R. Degl'Innocenti, S. Reidt, A. Guarina, D. Rezzonico, G. Poberaj, and P. Gunter, "Micromachining of ridge optical waveguides on top of He-implanted β -BaB₂O₄ crystals by femtosecond laser ablation," *J. Appl. Phys.* **100**(11), 113121 (2006).
25. A. Ródenas, G. A. Torchia, G. Lifante, E. Cantelar, J. Lamela, F. Jaque, L. Roso, and D. Jaque, "Refractive index change mechanisms in femtosecond laser written ceramic Nd:YAG waveguides: micro-spectroscopy experiments and beam propagation calculations," *Appl. Phys. B* **95**(1), 85–96 (2009).
26. A. Ródenas, D. Jaque, C. Molpeceres, S. Lauzurica, J. L. Ocaña, G. A. Torchia, and F. Agulló-Rueda, "Ultraviolet nanosecond laser-assisted micro-modifications in lithium niobate monitored by Nd³⁺ luminescence," *Appl. Phys., A Mater. Sci. Process.* **87**(1), 87–90 (2007).
27. R. Ramponi, R. Osellame, and M. Marangoni, "Two straightforward methods for the measurement of optical losses in planar waveguides," *Rev. Sci. Instrum.* **73**(3), 1117–1120 (2002).
28. J. F. Ziegler, computer code, SRIM <http://www.srim.org>.
29. J. Siebenmorgen, K. Petermann, G. Huber, K. Rademaker, S. Nolte, and A. Tünnermann, "Femtosecond laser written stress-induced Nd:Y₃Al₅O₁₂ (Nd:YAG) channel waveguide laser," *Appl. Phys. B* **97**(2), 251–255 (2009).

1. Introduction

As one of the most excellent gain media for solid state lasers, the neodymium doped gadolinium gallium garnet (Nd:Gd₃Ga₅O₁₂ or Nd:GGG) has attracted much attention owing to its outstanding optical advantages and thermal properties [1, 2]. The waveguide geometry could confine light propagation in extremely small volumes of the dimensional order of several micrometers, in which higher optical intensities could be obtained in respect to the bulks. Consequently, lower lasing thresholds and comparable efficiencies of the laser generation in waveguides could be achieved owing to the specific features of the structures [3]. The combination of the ability for on-chip integration makes waveguide laser devices particularly useful in integrated photonic and modern optical communication systems [4–6]. For practical applications, two dimensional (2D) waveguides (typically in channel or ridge configurations) are more attractive than one dimensional (1D) structures (such as planar and slab waveguides) owing to the more compact geometry in 2D guiding structures that stronger spatial confinement of light achieved while reducing the cost of substrate materials [7–9].

Several techniques have been utilized to fabricate waveguides in optical crystals, however, only the physical methods, such as ion implantation [10, 11] femtosecond laser inscription [12] and proton beam writing [13] are applicable to Nd:GGG for waveguide fabrication due to its stable chemical properties. Recently, the irradiation of swift heavy ions (i.e., with energy higher than 1MeV/amu) has emerged to be a powerful technique to fabricate waveguides in a couple of optical materials [14–20]. The normal light ion implantation creates negative refractive index layer buried the end of the ion track via nuclear collisions, constructing so called "barrier" waveguide [8–11, 21, 22]. Compared to the normal ion implantation, the swift ion beams modify the refractive index of the substrates mainly through the electronic excitation induced damages rather than the nuclear collisions. In such cases, the refractive index modification mainly happens during most path of the incident ions' trajectory via the impact of amorphous or highly defective nanotracks from a single ion or the overlap of a few ions [9, 14–18]. The advantages include the much reduced irradiation fluences and larger refractive index contrast with respect to the bulk, etc. Successful examples of swift heavy ion irradiate planar waveguides include α -SiO₂ [14], LiNbO₃ [15, 16], Nd:YCOB [17], Nd:YAG [18], and KGd(WO₄)₂ [19]. In order to form a 2D waveguide, a ridge structure is

advantageous for more compact lateral confinement of light fields. The femtosecond (fs) laser ablation technique has become increasingly attractive in recent years owing to the various practical applications in microstructuring of various materials [23]. For example, it has been applied to produce ridge waveguide structures on the surface of β -BaB₂O₄ nonlinear waveguide [9, 24]. In this work, we report on the fabrication of ridge waveguide in Nd:GGG crystals by combining swift carbon ion irradiation and femtosecond laser ablation, and the realization of waveguide lasers at wavelength of 1.06 μ m.

2. Experiments in details

The Nd:GGG crystal (doped by 1 at. % Nd³⁺ ions) was obtained from Atom Optics Co. Ltd, Shanghai, China. It was cut with the size of $5 \times 5 \times 2$ mm³ and optically polished. In the first step, the carbon (C⁵⁺) ions at energy of 17 MeV and fluence of 2×10^{14} ions/cm² were irradiated on one of the sample surfaces (5×5 mm²) to form a planar waveguide layer by utilizing the 3MV tandem accelerator at Helmholtz-Zentrum Dresden-Rossendorf, Germany. The ion current density was kept at a low level (about 6-8 nA/cm²) to avoid the heating and charging of the sample. And then, on top of the irradiated surface (i.e., the planar waveguide surface), we used a Ti:Sapphire laser system, which delivered 120 fs pulses, linearly polarized at 796 nm and with a repetition rate of 1 kHz, to microstructure the ridge structures. The laser beam was focused by a $20 \times$ microscope objective (N.A. = 0.6), and the sample was located at a XYZ motorized stage with a spatial resolution of 0.2 μ m. The linear focus of the objective was located on the irradiated surface of the sample and the pulse energy was set to 4.2 μ J. As a consequence, two grooves were ablated with lateral separation of 35 μ m by the laser scanning at a translation velocity of 50 μ m/s. With the lateral confinement of microstructured grooves and vertical restriction of ion irradiated planar waveguide, the ridge waveguide was produced in Nd:GGG crystal.

We used a fiber-coupled confocal microscope (Olympus BX-41) to measure the microphotoluminescence (μ -PL) properties of the Nd:GGG planar waveguide at room temperature. A 10-mW continuous wave (cw) radiation from an argon laser at a wavelength of 488nm was focused onto the surface of the sample by utilizing a $100 \times$ objective with numerical aperture N.A. = 0.95, exciting the transition of Nd³⁺ ions through $^4I_{9/2} \rightarrow ^2G_{3/2}$ [25, 26]. Then, the subsequent $^4F_{3/2} \rightarrow ^4I_{9/2}$, $^4I_{11/2}$ emission generated from Nd³⁺ ions was collected by utilizing the same microscope objective and, after passing through a confocal aperture, analyzed by a CCD camera attached to a high resolution fiber-coupled spectrometer.

We performed the end-face coupling experiment at 632.8 nm to characterize the modal profiles of the guided modes. The propagation loss for the planar waveguide was ~ 2 dB/cm at 632.8 nm; for the ridge waveguide, the propagation loss was determined to be ~ 4.5 dB/cm at 632.8 nm. In both cases, we used the back-reflection method [27]. The higher attenuation for ridge waveguide should be partly attributed to the non-perfect side-walls fabricated by the fs lasers. The roughness of the side walls was estimated to be ~ 500 nm by the SEM image.

The waveguide laser operation experiment was performed by utilizing an end pumping system. A polarized light beam at a wavelength of 808 nm was generated from a tunable cw Ti:Sapphire laser (Coherent MBR 110) at room temperature. A spherical convex lens with focus length of 25 mm was used to couple the laser beam into the planar waveguide. An input mirror (with the transmission of 98% at 808 nm and the reflectivity $>99\%$ at ~ 1064 nm) and an output mirror (with the reflectivity $>99\%$ at 808 nm and the transmittance of 60% at ~ 1064 nm, respectively) were adhered to the input and output end face of the planar waveguide respectively, forming the Fabry-Perot lasing resonator cavity. The generated waveguide laser was collected by utilizing a $20 \times$ microscope objective lens (numerical aperture N.A. = 0.4) and imaged by using an infrared CCD. We used a spectrometer with resolution of 0.2 nm to analyze the emission spectra of the laser beam from the waveguide.

3. Results and discussion

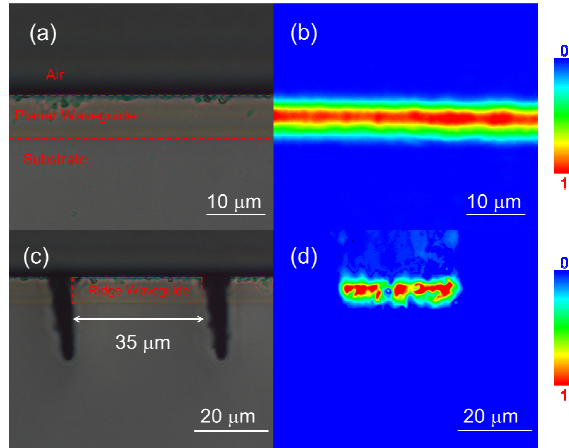


Fig. 1. The microscope image of the end face of the Nd:GGG (a) planar waveguide and (c) ridge waveguide (the dashed lines indicate the waveguide regions); and the near-field modal profiles of the (b) planar and (d) ridge waveguides at the wavelength of 632.8 nm.

Figure 1(a) shows the microscope image of the end face of 17 MeV C^{5+} ion irradiated Nd:GGG planar waveguide. It can be clearly seen that the ion beam modified region of the Nd:GGG is with a thickness of $\sim 8 \mu\text{m}$, which is in good agreement with the mean projected range of the 17 MeV C^{5+} ions in the Nd:GGG crystal calculated by the SRIM 2010 (Stopping and Range of Ions in Matter) code [28]. Figure 1(c) depicts the cross section of the ridge waveguide produced by femtosecond laser ablation of the 17 MeV C^{5+} ion irradiated Nd:GGG. The ridge waveguide is located in the region of the planar waveguide between the two micromachined grooves by the fs-laser ablation. Figures 1(b) and 1(d) show the near field intensity images from the Nd:GGG planar and ridge waveguide at 632.8 nm, respectively.

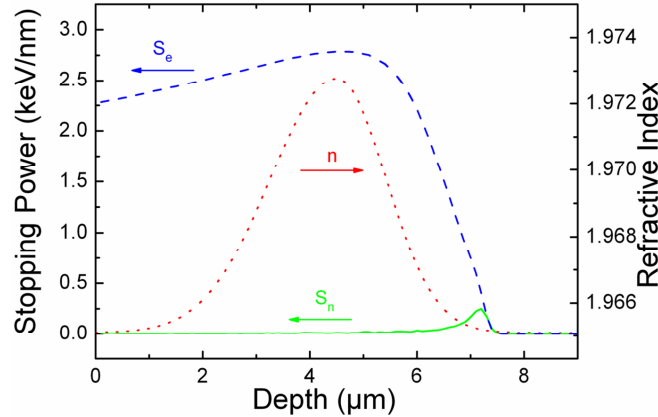


Fig. 2. The electronic stopping power (blue dashed line), nuclear stopping power (green solid line) curves as well as the refractive profile of the waveguide (red dotted line) as a function of the depth from the sample surface.

The modification of the refractive index in the waveguide layer was estimated by measuring the N. A. of the waveguide. The maximum refractive index increase (Δn) was calculated to be $\Delta n \approx +0.008$ by using the formula

$$\Delta n = \frac{\sin^2 \Theta_m}{2n} \quad (1)$$

where θ_m is the maximum incident angular deflection at which no transmitted power change occurs, and $n = 1.9651$ is the refractive index of the unmodified substrate [29]. The electronic and nuclear stopping power (S_e and S_n) profiles of 17 MeV C^{5+} ion in Nd:GGG crystals (as shown in Fig. 2) was obtained by using the SRIM 2010 code. As one can see, the values of S_e are obtained within the first 0-8 μm , overwhelmingly dominating over S_n , which suggests that the waveguide is mainly induced by the electronic damage.

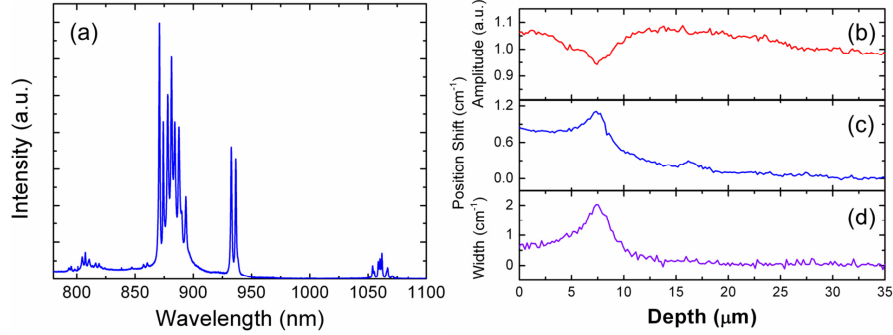


Fig. 3. (a) The room temperature luminescence emission spectrum correlated to Nd^{3+} ions at ${}^4F_{3/2} \rightarrow {}^4I_{9/2}$ transition of the Nd:GGG crystal, (b) the emitted intensity, (c) spectral shift and (d) emission width (at FWHM) of the 932.7 nm emission line.

Figure 3(a) shows the room-temperature PL emission spectrum of the Nd^{3+} ion in Nd:GGG crystal. For detailed understanding of the modification of the C^{5+} ions beams on the fluorescence properties of the planar waveguides, we focused on the hyper-sensitive emission line at 932.7 nm. Figures 3(b), 3(c), and 3(d) depict the 1D μ -PL profiles based on the spectral intensity, spectral shift and spectral broadening of this line, respectively. As we can see, the intensity of fluorescence signals decreases by about 10% in the waveguide with respect to the bulk, which means the majority of the PL active features has been preserved, without clear quenching. Nevertheless, the peak position shifts by 1.1 cm^{-1} , and the emission line is broadened by maximally 2 cm^{-1} , suggesting the obvious modification of the Nd:GGG fluorescence emission properties. It is reasonable to assume that the μ -PL features of the ridge waveguide is similar to those of the planar one, since the fs-laser ablation does not induce any induction of defective effects in the waveguide regions.

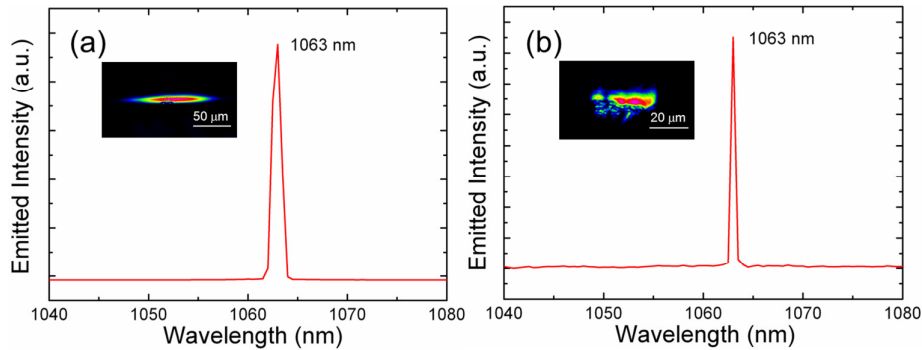


Fig. 4. Laser emission spectra from the Nd:GGG (a) planar waveguide and (b) ridge waveguide. The insets depict the laser modal profiles at lasing wavelength of $\sim 1063 \text{ nm}$.

Figures 4(a) and 4(b) depict the laser emission spectra from 17 MeV C^{5+} ions irradiation Nd:GGG planar waveguide and ridge waveguide fabricated by femtosecond laser ablation after 17 MeV C^{5+} irradiation, respectively, when the absorbed power is above the oscillation threshold. The central wavelength of the laser emission from the planar and ridge waveguides

are ~ 1063 nm, which is corresponding to the main fluorescence of ${}^4F_{3/2} \rightarrow {}^4I_{11/2}$ transition of Nd^{3+} ions.

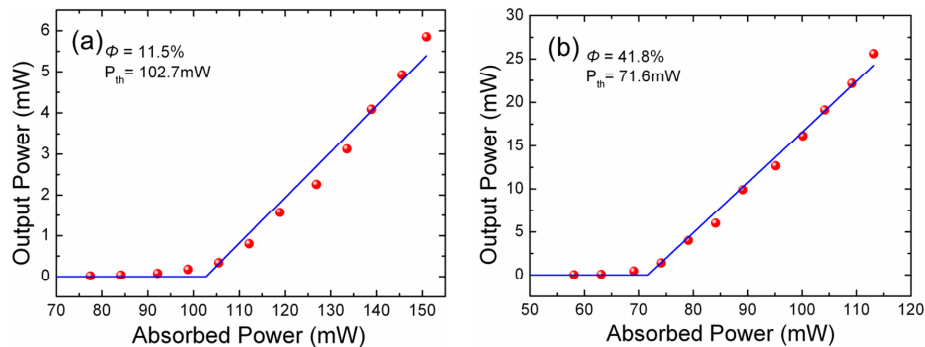


Fig. 5. Output laser power at 1063 nm as a function of absorbed pump power at 808 nm obtained from (a) the Nd:GGG planar waveguide and (b) the Nd:GGG ridge waveguide.

Figures 5(a) and 5(b) show the output laser power (at wavelength of 1063 nm) as a function of the 808 nm absorbed power generated in the Nd:GGG planar and ridge waveguide at room temperature. The absorbed power was calculated with the reasonable consideration of the coupling efficiency of the pump beam, transmittance and reflectivity of the optical elements in the system [11]. From the linear fit of the experimental data, we have determined that the lasing thresholds are 102.7 mW and 71.6 mW for Nd:GGG planar and ridge waveguides, respectively. And the slope efficiencies are 11.5% and 41.8%, respectively. As the absorbed pump powers increase, the output laser power of these two waveguides climbed to maximums at 5.9 mW and 25.6 mW at absorbed pump powers of 151 mW and 113 mW, corresponding to optical conversion efficiency of 4% and 23%, respectively. With comparison of Figs. 5(a) and 5(b), one can clearly conclude that the ridge waveguide is with much better performance than the planar one, resulting in reduced lasing threshold, higher slope efficiency and output laser power. It should be pointed that the better laser performance of the ridge waveguide may be further improved by smoothing the side walls (reducing the roughness) by additional processing (e.g., ion beam sputtering [24]). Nevertheless, these results indicate that the fs-laser micromachined ridge waveguide structures are ideal platform for integrated laser generations in Nd:GGG crystal.

4. Summary

We have reported on the fabrication of optical ridge waveguide in Nd:GGG laser crystals, using swift C^{5+} ion irradiation and fs laser ablation. The waveguide was formed in the electronic damage region, which confined laterally by two fs laser ablated air grooves. The $\mu\text{-PL}$ properties of the bulk were well preserved in the waveguide regions. The cw ridge waveguide laser at 1063 nm was realized with a lasing threshold of 71.6 mW and a slope efficiency of 41.8%, which exhibits a superior laser performance to the planar configuration. This work has shown the femtosecond laser ablation technique combined with swift heavy ion irradiation may be an effective method to fabricate active ridge waveguides as laser sources.

Acknowledgments

The work is supported by the National Natural Science Foundation of China (No. 10925524), Specialized Research Fund for the Doctoral Program of Higher Education of China under Grant 20090131110016, the Spanish Ministerio de Ciencia e Innovación (MICINN) through Consolider Program SAUUL CSD2007-00013 and project FIS2009-09522. S.Z. acknowledges the funding by the Helmholtz-Gemeinschaft Deutscher Forschungszentren (HGF-VH-NG-713). Support from the Centro de Láseres Pulsados (CLPU) is also acknowledged.